Photoinduced phase separation in $Bi_{0.4}Ca_{0.6}MnO_3$ thin films

V. N. Smolyaninova, E. Talanova, R. Kennedy, Rajeswari M. Kolagani, M. Overby, L. Aldaco, G. Yong, and K. Karki
Department of Physics, Astronomy and Geosciences, Towson University, Towson, Maryland 21252, USA
(Received 4 February 2007; revised manuscript received 21 June 2007; published 21 September 2007)

In this paper, we report a study of photoinduced and current-induced resistivity changes in $Bi_{0.4}Ca_{0.6}MnO_3$ thin films. The photoinduced effects were investigated using both far-field and near-field optical techniques. It was found that substrate-induced strain affects the stability of the charge ordering. The magnitude of the energy barrier separating the metastable conducting phase and the charge-ordered insulating phase estimated from the temperature dependence of the lifetime of the photoinduced conducting phase was found to be large, of the order of the charge-ordering temperature.

DOI: 10.1103/PhysRevB.76.104423 PACS number(s): 75.47.Lx, 71.30.+h, 78.20.−e, 64.75.+g

I. INTRODUCTION

Doped rare-earth manganites $R_{1-x}A_xMnO_3$ (R being a trivalent rare earth and A being a divalent alkaline-earth ion) exhibit a wide variety of physical phenomena due to complex interplay of electronic, magnetic, orbital, and structural degrees of freedom. One of the most intriguing properties of manganites is the coexistence of two (or several) distinct electronic phases.[1–6] Different competing phases, such as phases with different magnetic ordering, charge-ordered and disordered phases, or metallic and insulating electronic phases, can coexist for certain compositional and temperature ranges, or when material is influenced by external stimuli, such as magnetic field, electric field, or electromagnetic wave irradiation.[1,7–9] A photoinduced insulator-to-metal transition in manganese oxides is especially interesting from the point of view of creating photonic devices, such as photonic band-gap materials with periodically modulated refractive index.[8,10,11] A high refractive index contrast between the photoinduced conducting and insulating charge-ordered phases promises to be sufficient for the development of a photonic crystal material. An important point for the development of manganite-based photonic devices is the possibility of coexistence of two phases with high refractive index contrast on a submicron scale, in this case charge-ordered insulating and charge-disordered metallic phases. From this perspective, it is important to understand the physics of photoinduced conductive and insulating charge-ordered phase coexistence in manganites, its dynamics, and its stability.

Since estimated penetration depth of visible light is about 300 nm, charge-ordered material in thin film form is preferable for such study. Previously, we reported large photoinduced resistivity changes in $Bi_{0.4}Ca_{0.6}MnO_3$ thin films associated with melting of the charge ordering by visible light.[11] Films grown under small compressive strain exhibited the largest photoinduced resistivity changes. In this paper, we report a study of photoinduced and current-induced resistivity changes and photoinduced reflectivity changes created and imaged by near-field scanning optical microscope (NSOM) in $Bi_{0.4}Ca_{0.6}MnO_3$ thin films grown under different types of substrate-induced strain. Samples grown on different substrates exhibit qualitatively similar photoinduced and current-induced resistivity changes. The magnitude of these changes and the charge-ordering temperature depend on strain. We investigated photoinduced phase coexistence and the dynamics of it, which allowed us to estimate the energy barrier separating the charge-ordered phase and the photoinduced conductive phase and to relate the size of the barrier and the size of the phase-separated regions to theoretical predictions.

II. EXPERIMENT

Thin films were grown by the pulsed laser deposition technique from a commercial polycrystalline target with nominal composition of $Bi_{0.4}Ca_{0.6}MnO_3$. The film thicknesses were around 50 nm. The substrates used were (100) oriented $LaAlO_3$ (LAO), which has a pseudocubic crystallographic structure with $a=3.79$ Å, (100) oriented $SrTiO_3$ (STO) with $a=3.905$ Å of a cubic structure, and (100) and (001) oriented $NdCaAlO_4$ (NCAO), which has a tetragonal structure. In-plane lattice parameter of (001) oriented NCAO is 3.685 Å, but (100) oriented NCAO has two different in-plane lattice parameters: $c=12.12$ Å and $b=3.685$ Å. The laser energy density on the target was about 1.7 J/cm^2, and the pulse repetition rate was 10 Hz. The LAO and NCAO substrates were kept at a constant temperature of 800 °C during the deposition. The deposition was carried out at a pressure of 400 mTorr of flowing oxygen. After deposition, the samples were slowly cooled to room temperature at a pressure of 400 Torr of oxygen. θ-2θ scans showed that films were single phase, and φ scans confirmed epitaxiality. The width of rocking curves, 0.04° for films grown on LAO and 0.2° for films grown on NCAO, shows good crystallinity of these films.

Direct current (dc) resistivity was measured by a four-probe method: constant dc current was passed through the sample via the outer contacts, and voltage was measured using the inner contacts. For sample illumination, we used a continuous argon-ion laser with 514, 488, 476, and 457 nm wavelengths, which has maximum power of 140 mW in multiline mode. Light-induced resistivity changes in $Bi_{0.4}Ca_{0.6}MnO_3$ thin films were measured in four-in-line electrical contact configuration, as shown in Fig. 3 (inset). The distance between voltage contacts was approximately 0.3 mm. The space between voltage contacts was illuminated with full power (140 mW) multiwavelength (514, 488, 476,

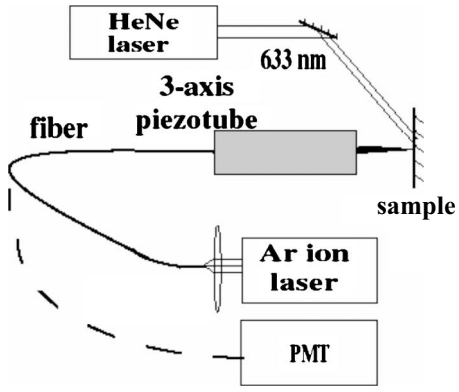

FIG. 1. Schematic view of our near-field optical experimental setup.

and 457 nm) argon-ion laser light (if not indicated otherwise). The laser beam was slightly focused with a 100 mm focal length lens, producing an illuminated region on the sample of approximate diameter of 0.05 mm and power density at the illuminated region of approximately 10^4 W/cm^2. Some measurements were done with 633 nm wavelength light of He-Ne laser of fixed 20 mW power.

NSOM was used to record local photoinduced reflectivity changes. The schematic view of our near-field optical experimental setup is presented in Fig. 1. The experiments were conducted at room temperature. The beam from the argon-ion laser was coupled into a single-mode optical fiber, which was tapered to form a 50 nm diameter uncoated tip. The microscope tip was attached to a piezotube that scanned it over the sample surface while keeping the tip-sample distance constant by means of shear force feedback. The sample topography was measured with nanometer resolution by recording the feedback signal. The sample was illuminated from the side by weak 633 nm probe light from a He-Ne laser. The 633 nm light reflected by the sample surface was collected by the microscope tip and directed to a photomultiplier (PMT) by the same fiber. This was done before and after local sample exposure to 488 nm/514 nm light through the same fiber via 3 dB coupler. Thus, simultaneous measurements of the sample topography and surface reflectivity at 633 nm were performed.

III. RESULTS AND DISCUSION

A. Influence of the substrate on the charge-ordering temperature

Figure 2 shows the temperature dependence of resistivity $\rho(T)$ for studied $Bi_{0.4}Ca_{0.6}MnO_3$ thin films and for the bulk target. At the charge-ordering transition, the temperature dependence of the resistivity has a kink (a change in derivative) in bulk samples.[12] Our target material has the charge-ordering temperature (T_{CO}) of 330 K, which is consistent with data reported elsewhere.[12] The rise of resistivity at the charge-ordering temperature in thin films is not as sharp as observed in the bulk material, as was noted previously.[11,13] There are indications that substrate-induced strain plays a key role in reducing the sharpness of the transition.[14] It was

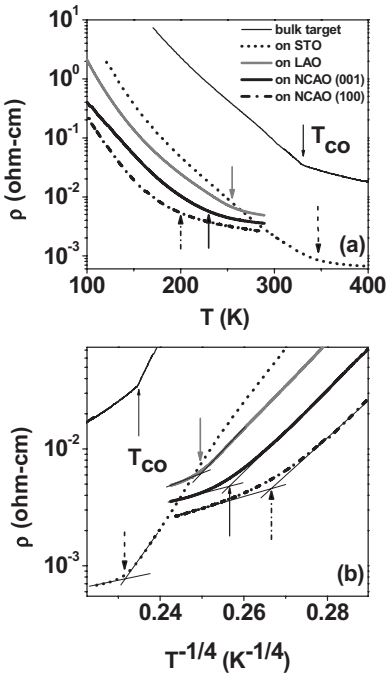

FIG. 2. (a) Temperature dependence of the resistivity of $Bi_{0.4}Ca_{0.6}MnO_3$ polycrystalline target and thin films grown on different substrates. (b) Temperature dependence of the resistivity plotted as $\ln \rho(T^{-1/4})$. Solid lines follow low and high temperature linear ranges and their crossing at the charge-ordering temperatures. The charge-ordering temperatures are indicated with the arrows.

shown previously that $\ln \rho$ vs $T^{-1/4}$ plot has a low temperature linear range crossing over to high temperature linear range at the charge-ordering temperature for the $Bi_{1-x}Ca_xMnO_3$,[12] possibly reflecting the Mott variable range hopping process in these materials.[12,15] We use this empirically useful method to determine the approximate (since the transition is wide) charge-ordering temperature [Fig. 2(b)]. The so obtained charge-ordering temperatures for thin films grown on LAO and NCAO are lower than for the bulk: T_{CO}=256, 230, and around 200 K for films grown on LAO, (001) oriented NCAO, and (100) oriented NCAO, respectively. The films grown on STO, on the other hand, have the charge-ordering temperature higher than the bulk: T_{CO} =347 K. Our x-ray scattering studies on these films show the presence of superlattice peaks associated with charge ordering below charge-ordering temperatures consistent with the T_{CO} determined from the resistivity measurements.[16]

Large substrate-related difference in the charge-ordering temperatures indicates the influence of strain on the charge ordering in thin films of $Bi_{1-x}Ca_xMnO_3$. The lattice parameters of STO, LAO, and (001) oriented NCAO are 3.905, 3.79, and 3.685 Å, respectively, while corresponding lattice parameter for $Bi_{0.4}Ca_{0.6}MnO_3$ is $V^{1/3}$=3.81 Å.[17] Therefore, films grown on LAO and (001) oriented NCAO are expected to be under compressive strain, while films grown on STO are expected to be under tensile strain. Indeed, the differences in the out-of-plane lattice constants clearly reveal the differences in the strain states of the films: 3.74 Å for the films grown on STO, 3.80 Å for the films grown on LAO, 3.82 Å for the films grown on (001) oriented NCAO, and

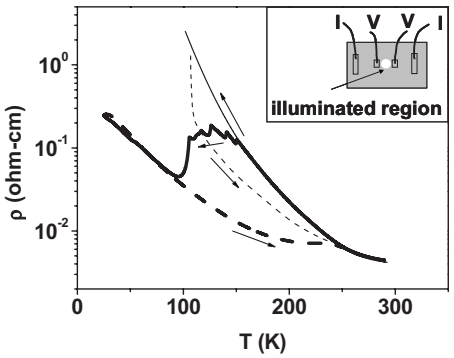

FIG. 3. Temperature dependence of the resistivity of the $Bi_{0.4}Ca_{0.6}MnO_3$ thin film grown on LAO: thin solid line, taken on cooling without illumination; thin dashed line, taken on warming with illumination; thick solid line, taken on cooling with illumination; thick dashed line, taken on warming with illumination. Arrows indicate cooling or warming for each curve. The inset shows experimental current and voltage contact configuration with respect to illuminated region.

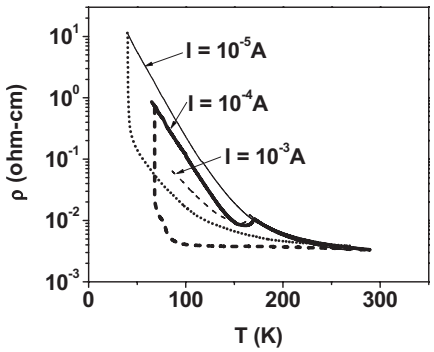

FIG. 4. Temperature dependence of the resistivity of the $Bi_{0.4}Ca_{0.6}MnO_3$ thin film grown on (100) oriented NCAO substrate: thin solid line, taken on cooling without illumination with $I=10^{-5}$ A; thick solid line, taken on cooling without illumination with $I=10^{-4}$ A; thin dashed line, taken on cooling without illumination with $I=10^{-3}$ A; dotted line, taken on warming with illumination with $I=10^{-5}$ A; thick dashed line, taken on warming with illumination with $I=10^{-4}$ A.

3.77 Å for the films grown on (100) NCAO. In-plane tensile (compressive) strain leads to the expansion (compression) of the out-of-plane lattice constants. Compressive strain seems to reduce the charge-ordering temperature: the T_{CO} is smaller for the case of (001) oriented NCAO substrate, which provides larger lattice mismatch than LAO. In contrast, a tensile strain introduced by STO substrate tends to increase the charge-ordering temperature of $Bi_{1-x}Ca_xMnO_3$ thin films compared with bulk T_{CO}, as we reported previously.[11] However, the largest change in the charge-ordering temperature with respect to bulk was found in (100) oriented NCAO substrate. This substrate introduces a nonuniform strain: compressive in one in-plane direction ($b=3.685$ Å is smaller than the bulk value of 3.81 Å) and tensile in the other in-plane direction ($c/3=4.033$ Å is larger than the bulk value). It seems that such nonuniform strain weakens the charge ordering further, which lowers the charge-ordering temperature more than in the case of a uniform compressive strain. A detailed study of strain effects on charge ordering in $Bi_{1-x}Ca_xMnO_3$ films will be published elsewhere.[18]

B. Thermal history dependence of photoinduced changes

Photoinduced resistivity changes in the $Bi_{0.4}Ca_{0.6}MnO_3$ thin films depend strongly on thermal history. Figure 3 shows path dependence of the photoinduced changes for the sample grown on LAO substrate. If the sample is first cooled down to the temperature of around 100 K and then illuminated with full power (140 mW) multiwavelength argon-ion laser light, its resistivity decreases by about 1 order of magnitude (Fig. 3), as was previously found.[11] During the subsequent warming, the resistivity under illumination (Fig. 3, thin dashed curve) is smaller than the resistivity without illumination (Fig. 3, thin solid curve). The situation is very different if the sample is cooled with illumination on (Fig. 3, thick solid curve.) Above approximately 150 K, the resistivity of the illuminated sample is identical to the resistivity of the sample without illumination. However, as temperature decreases below $T=150$ K, the resistivity of illuminated sample starts to drop, suddenly experiencing the series of jumps. On warming, the resistivity changes smoothly, without sudden changes (Fig. 3, thick dashed curve), and has values much lower than for the warming run, where the sample was initially cooled without illumination (Fig. 3, thin dashed curve). Above the charge-ordering temperature, illumination has no effect on the resistivity of the sample. Repeated runs did not lead to exact repetition of the same curve for the warming with illumination, i.e., the jumps could occur at different temperatures and have different magnitudes, but the general behavior remained the same: jumplike changes in resistivity resulting in values much lower than for the warming run taken after initial cooling without illumination. The current used in these measurements was sufficiently small to avoid current-induced resistivity changes reported in Sec. III C.

Samples grown on different substrates exhibit qualitatively similar path dependence of the photoinduced resistivity changes. The magnitude of photoinduced changes is largest for the films grown on (100) oriented NCAO substrate (Fig. 4, $I=10^{-5}$ A) and smallest for films grown on STO [Fig. 8(d)].

Such path dependence of the photoinduced changes gives an insight into the process of destruction of the charge-ordered phase by light. On cooling with illumination, photoinduced changes start to occur at a temperature around 150 K. Measurements of the optical conductivity of these materials show that conductivity decreases with temperature at the energies of Ar-ion laser light.[19] Therefore, the penetration depth of light of these wavelengths increases when temperature decreases. This could facilitate the formation of photoinduced conducting phase in large volume of the sample at low temperatures. It is known that the insulator-to-metal transition in manganites can be of percolative origin.[2,3,20] Probably, isolated regions of a conducting photoinduced phase may even exist at the temperatures above 150 K, but we do not see a decrease in resistivity because there is no percolation yet. As the temperature decreases,

light can create a large amount of the conducting phase and the percolation occurs, producing a significant photoinduced effect. If afterward, on warming above 150 K, the percolative channels remain open, the photoinduced resistivity reduction persists up to the charge-ordering temperature, accounting for the difference in resistivity between the cooling and warming runs. It was found that the transition between the charge-disordered conductive phase and the charge-ordered insulating phase has martensitic character.[21] A rapid growth (or reduction) of a martensitic phase at fixed temperature as well as strong hysteresis are two of the characteristic features of the martensitic phase transformations.[22] The fact that the largest photoinduced changes occur in the films grown on (100) oriented NCAO substrate (the most strained films) is also consistent with martensitic character of the phase transformation, which are favored by the external strain. Thus, the light-induced transformation of the charge-ordered phase can have martensitic and percolative character.

C. Current-induced and photoinduced effects in the $Bi_{0.4}Ca_{0.6}MnO_3$ thin films

As was shown previously, current (electric field) can destroy the charge ordering,[7] or stabilize the conducting phase[8] in charge-ordered manganites. Effects of current (electric field) in the charge-ordered films were also studied, showing that current can destroy or weaken the charge ordering, leading to a more conductive state and nonlinear and hysteretic *I-V* characteristics.[15,23,24] We have carried out the study of the combined effect of current and illumination on the $Bi_{0.4}Ca_{0.6}MnO_3$ thin film grown on different substrates.

Figure 4 shows the temperature dependence of the resistivity of the $Bi_{0.4}Ca_{0.6}MnO_3$ thin film grown on (100) oriented NCAO substrate measured using different currents with and without illumination. The cross-sectional area of the sample for this measurement was $0.25\times(5\times10^{-6})$ cm^2. The increase of the current does not have much effect on the resistivity above the temperature of approximately 170 K. Below this temperature, resistivity decreases suddenly, resembling the photoinduced jumplike changes in resistivity on cooling with illumination. On further cooling, the resistivity values are smaller for larger currents, and around $T=100$ K, the resistivity measured using current of 10^{-3} A is approximately 1 order of magnitude smaller than the resistivity measured using current of 10^{-5} A.

The semiconducting behavior of the $R(T)$ with illumination measured with $I=10^{-5}$ A indicates the presence of the charge-ordered insulating phase that was not completely destroyed by illumination, when current is low. However, when current is 10^{-4} A, the resistivity drops by 2 orders of magnitude with illumination (Fig. 4) and changes very weakly on warming, having the value of approximately room-temperature resistivity. With illumination, the increase of current beyond 10^{-4} A does not produce further reduction of resistivity. This indicates a complete destruction of the charge ordering in this film by combined application of illumination and current, while the application of one of these factors separately was not sufficient to produce such effect.

Since the current is able to destroy the charge ordering in this material, the voltage-current (*V-I*) dependences are

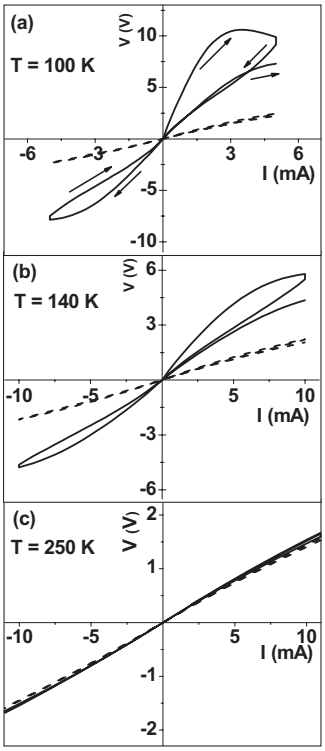

FIG. 5. Voltage-current dependences for the $Bi_{0.4}Ca_{0.6}MnO_3$ thin film grown on (001) oriented NCAO substrate with illumination (dashed curves) and without illumination (solid curves) for different temperatures: (a) $T=100$ K, (b) $T=140$ K, and (c) $T=250$ K. The sample was current biased. Arrows indicate the direction of increase or decrease of current.

nonlinear. The voltage-current dependences for the $Bi_{0.4}Ca_{0.6}MnO_3$ thin film grown on (001) oriented NCAO substrate are shown in Fig. 5. At low temperatures, *V-I* curves are strongly nonlinear and hysteretic [Fig. 5(a) and 5(b)], which points to the presence of two competing phases. They exhibit a region of negative differential resistance [Fig. 5(a)], which was observed previously in the charge-ordered manganites[7,15,24,25] and is not surprising if a new phase with higher conductivity is created. As current starts to increase from zero, the initial slope of the curve (resistance) is higher than for the curve measured in the negative current direction. Moreover, in the second run in the positive direction (after the full hysteresis loop is completed), the slope is also significantly smaller than in the initial run [Figs. 5(a) and 5(b)]. However, if the sample remains at zero current for several minutes, the *V-I* curve will follow the initial path with higher resistance. These *V-I* curves are also current ramp rate dependent: the faster ramp rate produces *V-I* curve with higher voltage for a given current value. Such history-dependent behavior can be explained by the following picture. As the charge ordering is destroyed by the current, the metastable regions of the conductive phase are created. The longer the high current is applied (slower current ramp rate), the larger these regions can grow, resulting in smaller resistance. When the current is reduced to zero, the material does not return immediately to the charge-ordered phase with high resistance, but exhibits smaller resistance values (smaller slopes

at zero current on the negative current run and on the second positive current run). At higher temperatures, the nonlinearity, hysteresis, and history-dependent effects of the *V-I* curves diminish, and above the charge-ordering temperatures, the material exhibits approximately Ohmic behavior [Fig. 5(c)].

The *V-I* curves measured with illumination are almost linear, do not exhibit hysteresis, and do not depend on the history (with respect to application of current) (Fig. 5). The current which was sufficient to induce strong changes in resistivity in the sample without illumination is unable to further reduce resistance of the illuminated sample. Probably, this happens because the insulating charge-ordered phase, which could be affected by this current, is no longer present under illumination. Neither light nor current has much effect above the charge-ordering temperature, confirming that light- and current-induced effects in these films are associated with modification of the charge-ordering phase.

The largest current-induced effects are in the films grown on (100) oriented NCAO substrate: smaller currents are needed to induce the nonlinearity of the *V-I* curves, or the reduction of resistivity at a given temperature. The films grown on (001) oriented NCAO substrate and on LAO exhibit smaller current-induced conductivity changes, and films grown on STO exhibit the smallest current-induced effects for similar range of parameters. This trend is similar to substrate dependence of the photoinduced resistivity changes. Such substrate dependence of current-induced effects is consistent with the reduction of the charge-ordering temperature for the films with compressive and nonuniform strain, where the charge order is probably weakened and easier to destroy.

Joule heating, as one of the reasons for the nonlinearity of *V-I* curves, needs to be addressed. Indeed, if the sample is heated, the resistivity will decrease, showing the reduction of the slope of the *V-I* curve. However, this would not explain sudden jumps in $R(T)$ taken with larger current (Fig. 4), history dependence, i.e., the difference between the first and the second run in the positive direction [Figs. 5(a) and 5(b)], and different degree to which current affects the films of the same thickness grown on different substrates. Therefore, non-Ohmic behavior of *V-I* curves cannot be explained by Joule heating alone. However, slight nonlinearity of the *V-I* curve at $T=250$ K [Fig. 5(c)] above the charge-ordering temperature could result from Joule heating.

As for distinguishing light-induced and heat-induced effects, we have addressed this issue in Ref. 11. We have eliminated significant heat-induced effects by comparing large photoinduced changes on one film with miniscule photoinduced changes on another film at the same power of the laser.

D. Time dependence of photoinduced changes

In order to better understand the dynamics of this phase coexistence, we studied the time dependence of resistivity of $Bi_{0.4}Ca_{0.6}MnO_3$ thin films after sample illumination was switched on and off at different temperatures. A study of time dependence of photoinduced changes in the thin film of $Bi_{0.4}Ca_{0.6}MnO_3$ on LAO is shown in Fig. 6. Figure 6(a) shows the relaxation behavior of the resistance at 140 K after illumination was switched on or off. These time dependences can be fitted to the exponential law $\Delta R \propto \exp(-t/\tau)$, where at $T=140$ K the time constants τ are 25 and 49 s for the exponential decrease and increase of the resistance, respectively. The time constants of such processes were determined for different temperatures on warming for the laser light power of 140 mW [Fig. 6(b)] and 20 mW [Fig. 6(b), inset]. The time constant corresponding to the process of transition to a

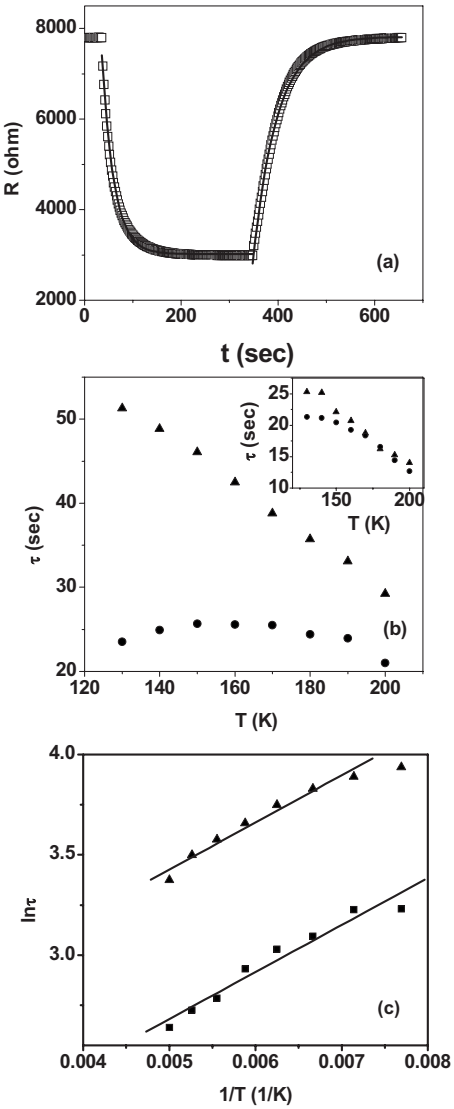

FIG. 6. (a) Time dependence of resistance of a $Bi_{0.4}Ca_{0.6}MnO_3$ film on LAO at $T=140$ K with illumination switched on and off for the laser light power of 140 mW. Solid lines are fits to the exponential time dependence $\Delta R \propto \exp(-t/\tau)$. (b) Temperature dependence of the time constants τ for the process of transition to a more conductive state after illumination was switched on (circles) and for the process of return to the original state after illumination was switched off (triangles) for the same film. The laser light power is 140 mW. The inset shows similar data for the laser light power of 20 mW. (c) Temperature dependence of the time constant plotted as $\ln \tau$ vs $1/T$ for the laser light powers of 140 mW (triangles) and 20 mW (squares). Solid lines are fits to the activation model.

more conductive state after illumination was switched on is smaller than the time constant for the process of return to the original state after illumination was switched off [Fig. 6(b)]. This difference increases with laser light power, and at low power, these time constants are close [Fig. 6(b), inset].

Under illumination, which partly destroys the charge ordering, the sample has more conductive charge-disordered phase. This phase is quasistable, i.e., has a substantial lifetime (characterized by a time constant τ) after the illumination is switched off: up to 2 min (for samples grown on NCAO substrate). Thus, for a considerable time, these two phases coexist without external stimuli. Such phase coexistence is possible because of the presence of two local energy minima corresponding to charge-ordered insulating and charge-disordered conducting phases in the energy landscape. In the temperature range from 120 to 200 K, the temperature dependence of the time constant can be approximated with an activation model [Fig. 6(c)]: $\tau \propto \exp(E/k_B T)$, where k_B is the Boltzmann constant and E is an energy barrier separating two local energy minima corresponding to charge-ordered insulating and charge-disordered conducting phases in the energy landscape. For the thin film of $Bi_{0.4}Ca_{0.6}MnO_3$ on LAO, E, the slope of the linear fit [Fig. 6(c)], is 235 K (20.3 meV). The value of the energy barrier is rather large, almost as large as the charge-ordering temperature (T_{CO}=256 K in this case). The value of the energy barrier is the same for the data taken with different (140 and 20 mW) laser light power.

The value of the energy barrier varies from 220 to 300 K depending on the substrate and the film thickness variation. However, E is always in the vicinity of the charge-ordering temperature. A linear fit in Fig. 6(c) is an approximation with a simple model of the processes that are, most probably, more complex. Deviation of the data from linear fit at low temperature could be due to slight nonexponentiality of the relaxation curves at these temperatures, which could be an indication of the presence of multiple energy barriers in the system at lower temperatures. Nevertheless, a simple activation model gives a quantitative estimate of the energy barrier separating two local energy minima corresponding to charge-ordered insulating and charge-disordered conducting phases in the energy landscape.

E. Intensity and wavelength dependence of the photoinduced changes

We have previously found that the lifetime of the photoinduced low-resistance state is increasing with the increase in intensity of the light almost linearly for the laser power up to 140 mW.[11] The magnitude of the photoinduced resistivity changes also increases with the increase of the light intensity (Fig. 7). The data were taken for the wavelengths of individual lines and multiline mode (514, 488, 476, and 457 nm with 514 and 488 nm lines making the largest contribution to the power) of argon-ion laser and for 633 nm wavelength of He-Ne laser. There is no significant difference in the photoinduced resistivity changes for different wavelengths for a studied power range (up to 50 mW, the maximum power of the singe line mode of our laser): the photoinduced resistivity changes produced by light of different wavelengths follow the same power dependence. The lifetime of the photoinduced low-resistance state also does not depend on the wavelength in our experimental range. The lifetime of the photoinduced low-resistance state[11] and the photoinduced resistivity changes do not exhibit the signs of saturation for the power densities up to approximately 5×10^4 W/cm^2, which corresponds to a power of 140 mW. This indicates that larger power density may induce larger photoinduced changes with a longer lifetime.

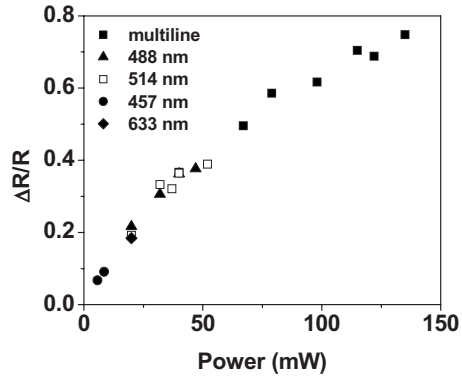

FIG. 7. Dependence of relative photoinduced resistivity changes on laser power for the $Bi_{0.4}Ca_{0.6}MnO_3$ film on LAO at T=100 K. Different wavelengths are shown by different symbols.

F. Photoinduced reflectivity changes

Recently, it was predicted that the energy landscape determines the scale of phase separation in manganites, with larger energy barriers corresponding to phase coexistence on a submicron scale, while smaller energy barriers lead to nanometerscale phase separation.[5] Since from our measurements of the temperature dependence of the lifetime we have found that the energy barrier is large, it would be interesting to study the size of different phases in phase-separated films of $Bi_{0.4}Ca_{0.6}MnO_3$.

We have performed this study using room-temperature NSOM. In this experiment, the microscope tip was initially positioned in the center of the field of view, and the sample was exposed for 20 s to about 140 mW of multiline argon-ion laser light through the microscope tip. The sample was illuminated from the side by weak nonresonant 633 nm light from a 5 mW He-Ne laser. Power density of this light is insufficient to produce any detectable photoinduced changes in the sample since the magnitude of photoinduced changes decreases with power. The 633 nm light reflected by the sample surface was collected by the microscope tip.

The $Bi_{0.4}Ca_{0.6}MnO_3$ on STO film was used for this study, since it has the charge-ordering temperature of 347 K, which is higher than room temperature. The photoinduced resistivity change for this sample is shown in Fig. 8(d). This change persisted at least up to 293 K (room temperature) with laser light on. The photoinduced resistivity change was not studied at higher temperature since we do not have an optical access in the high temperature setup. The magnitude of the photoinduced changes increases with the laser light power [Fig.

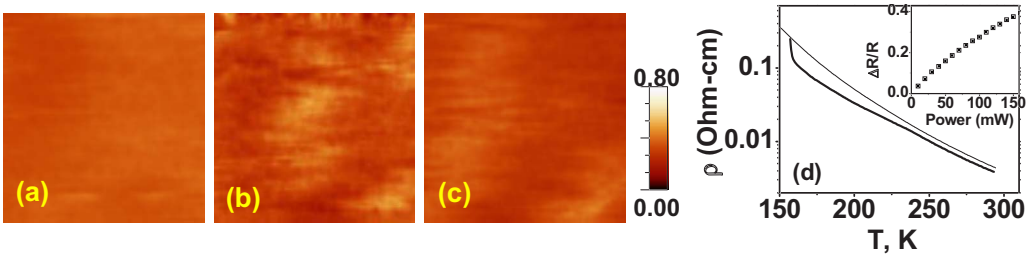

FIG. 8. (Color online) 1.7×1.7 μm^2 NSOM image of reflectivity of the $Bi_{0.4}Ca_{0.6}MnO_3$ film on STO (a) before illumination, (b) immediately after illumination, and (c) 7 min after illumination (described in text). Color (gray scale) indicator is given in arbitrary units. (d) Temperature dependence of the resistivity of the $Bi_{0.4}Ca_{0.6}MnO_3$ thin film grown on STO with illumination (thick line) and without illumination (thin line). Data were taken on warming. The inset shows the dependence of relative photoinduced resistivity changes on laser power at $T=270$ K.

8(d), inset]. Therefore, the magnitude of the photoinduced changes under the NSOM tip is expected to be much larger after illumination through the tip of the tapered fiber due to much larger power density of illumination (the estimated power densities are 5×10^6 W/cm^2 for NSOM measurements and 10^4 W/cm^2 for resistivity measurements).

Figure 8(a) shows a 1.7×1.7 μm^2 NSOM optical image before exposure to argon-ion laser light. The optical reflectivity of the sample is uniform. Topography corresponding to this optical image is, as expected, also flat (not shown). Figure 8(b) shows the NSOM optical image of the same area immediately after the exposure to argon-ion laser light. The image shows that submicron regions of increased reflectivity corresponding to a conducting charge-disordered phase have appeared. A field distribution of an uncoated fiber tip has a central maximum surrounded by concentric rings (ellipses) caused by the interference of multiple modes at the end of the tapered region. The geometry of the produced reflectivity pattern on the surface of the $Bi_{0.4}Ca_{0.6}MnO_3$ film is consistent with the complicated field distribution of an uncoated fiber tip: the regions of increased reflectivity appear not only at the center of the image, where the tip was positioned during illumination. However, the pattern of reflectivity changes on the surface of the $Bi_{0.4}Ca_{0.6}MnO_3$ film does not repeat the exact pattern of illumination: it does not have the shape of concentric rings or ellipses, as it would be the case if the phase-separated regions would be of the nanometer size. Therefore, it is probably more energetically preferable for this material to form large (submicron) regions of more reflective phase in the general locations of the maxima of illumination than to form nanoscale regions of more reflective phase, which would follow exactly the field distribution pattern of the tip.

The scan shown in Fig. 8(c) was taken immediately after the scan shown in Fig. 8(a). Therefore, there is approximately a 7 min time delay between the respective points of each scan due to scan time. Figure 8(c) shows that after approximately 7 min, the optical contrast diminishes because the sample relaxes back to its charge-ordered ground state. The lifetime of the photoinduced reflectivity changes (around 7 min) seems to be longer than the lifetime of the photoinduced resistivity changes (around 2 min). This can be explained by much larger power density used in NSOM for illumination than in the resistivity measurements and the fact that the lifetime of photoinduced changes increases with power, as we have shown in Ref. 11.

Thus, we have created a submicron phase coexistence of charge-ordered insulating phase [Figs. 8(b) and 8(c), darker regions] and conducting charge-disordered phase (lighter regions) by illuminating a $Bi_{0.4}Ca_{0.6}MnO_3$ thin film with visible light (~500 nm) through the tip of a NSOM. This is in agreement with theoretical prediction,[5] which links large energy barriers separating two phases and the submicron size of phase-separated regions.

IV. CONCLUSIONS

To summarize, charge-ordered epitaxial thin films of $Bi_{0.4}Ca_{0.6}MnO_3$ were grown on (100) and (001) oriented NCAO, LAO, and STO substrates, which subject these films to biaxial asymmetric, compressive, and tensile strain. Visible light illumination partly destroys the charge ordering in these materials, resulting in conductive and charge-ordered insulating phase coexistence. External stimuli (visible light illumination and current) can affect the charge ordering to a larger degree in films with nonuniform strain [grown on (100) oriented NCAO] followed by films with compressive strain. Combined effect of the illumination and current can destroy the charge ordering completely in films grown on (100) oriented NCAO. Nonuniform and compressive strain appears to weaken the charge ordering in $Bi_{0.4}Ca_{0.6}MnO_3$ films.

Photoinduced resistivity changes are hysteretic, depend on thermal history, and are characterized by abrupt drops of resistance if cooled under illumination. Such behavior is consistent with martensitic character of this phase transformation, where large regions of the conducting phase are created, and also could be indicative of percolative transport in the photoinduced conducting phase. The *V-I* curves are nonlinear and hysteretic and depend on history with respect to application of current. Current-induced effects are related to appearance of a new conducting phase when current increases and cannot be explained by Joule heating alone. Visible light illumination reduces resistivity and makes *V-I* curves for films on NCAO almost linear in the experimental range, which indicates the destruction of the charge ordering by combination of light and current.

Temperature dependence of the lifetime of the photoinduced conducting phase is consistent with a activation model, which allows us to evaluate the size of the energy barrier separating metastable conducting phase and charge-ordered insulating phase. This energy barrier is large, of the order of the charge-ordering temperature, i.e., the local energy minimum corresponding to conducting charge-disordered phase is deep. In order to study the size of the regions of photoinduced phase, we have created a phase coexistence of charge-ordered insulating phase and conducting charge-disordered phase by illuminating a $Bi_{0.4}Ca_{0.6}MnO_3$ thin film with visible light through the NSOM tip. The submicron size of the photoinduced regions of larger reflectivity is in agreement with theoretical prediction,[5] which links large energy barriers separating two phases and the submicron size of phase-separated regions.

ACKNOWLEDGMENTS

We acknowledge I. I. Smolyaninov for helpful discussions and S. Casey, D. Cox, D. Kent, and G. Vanmeter for experimental help. This work is supported by NSF Grants Nos. DMR-0348939, DMR-0453342, and DMR-04221141 and Research Corporation Grant No. CC 629.

[1] Myron B. Salamon and M. Jaime, Rev. Mod. Phys. **73**, 583 (2001).
[2] M. Uehara, S. Mori, C. H. Chen, and S.-W. Cheong, Nature (London) **399**, 560 (1999).
[3] L. Zhang, C. Israel, A. Biswas, R. L. Greene, and A. de Lozanne, Science **298**, 805 (2002).
[4] Ch. Renner, G. Aeppli, B.-G. Kim, Y.-A. Soh, and S.-W. Cheong, Nature (London) **416**, 518 (2002).
[5] K. H. Ahn, T. Lookman, and A. R. Bishop, Nature (London) **428**, 401 (2004).
[6] G. C. Millard, M. J. Calderon, and P. B. Littlewood, Nature (London) **433**, 607 (2005).
[7] A. Asamitsu, Y. Tomioka, H. Kuwahara, and Y. Tokura, Nature (London) **388**, 50 (1997).
[8] M. Fiebig, K. Miyano, Y. Tomioka, and Y. Tokura, Science **280**, 1925 (1998).
[9] V. Kiryukhin, D. Casa, J. P. Hill, B. Keimer, A. Vigliante, Y. Tomioka, and Y. Tokura, Nature (London) **386**, 813 (1997).
[10] I. I. Smolyaninov, V. N. Smolyaninova, C. C. Davis, B. G. Kim, S.-W. Cheong, and R. L. Greene, Phys. Rev. Lett. **87**, 127204 (2001).
[11] V. N. Smolyaninova, M. Rajeswari, R. Kennedy, M. Overby, S. E. Lofland, L. Z. Chen, and R. L. Greene, Appl. Phys. Lett. **86**, 071922 (2005).
[12] H. Woo, T. A. Tyson, M. Croft, S.-W. Cheong, and J. C. Woicik, Phys. Rev. B **63**, 134412 (2001).
[13] W. Prellier, Amlan Biswas, M. Rajeswari, T. Venkatesan, and R. L. Greene, Appl. Phys. Lett. **75**, 397 (1999).
[14] D. H. Kim, H. M. Christen, M. Varela, H. N. Lee, and D. H. Lowndes, Appl. Phys. Lett. **88**, 202503 (2006).
[15] S. Chaudhuri and R. C. Budhani, Phys. Rev. B **74**, 054420 (2006).
[16] C. S. Nelson, R. M. Kolagani, M. Overby, V. N. Smolyaninova, and R. Kennedy, J. Phys.: Condens. Matter **18**, 997 (2006).
[17] V. A. Bokov, N. A. Grigorian, and M. F. Bryzhina, Phys. Status Solidi **20**, 745 (1967).
[18] Rajeswari M. Kolagani, G. Yong, V. N. Smolyaninova, (unpublished).
[19] M. Rubhausen, S. Yoon, S. L. Cooper, K. H. Kim, and S.-W. Cheong, Phys. Rev. B **62**, R4782 (2000).
[20] V. Podzorov, M. Uehara, M. E. Gershenson, T. Y. Koo, and S.-W. Cheong, Phys. Rev. B **61**, R3784 (2000).
[21] V. Podzorov, B.-G. Kim, V. Kiryukhin, M. E. Gershenson, and S.-W. Cheong, Phys. Rev. B **64**, 140406(R) (2001).
[22] G. V. Kurdjumov and O. P. Maksimova, Dokl. Akad. Nauk SSSR **61**, 83 (1948).
[23] V. Ponnambalam, S. Parashar, A. R. Raju, and C. N. R. Rao, Appl. Phys. Lett. **74**, 206 (1999).
[24] S. Srivastava, N. K. Pandey, P. Padhan, and R. C. Budhani, Phys. Rev. B **62**, 13868 (2000).
[25] T. Wu and J. F. Mitchell, Appl. Phys. Lett. **86**, 252505 (2005).